

Silicon Drift Detectors

Gaurav Somani

CeNSE, IISc

February 28, 2021

Outline

Absorption efficiency (η)

- ▶ X-rays absorbed in Si generates e-h pairs
- ▶ Fraction of photons absorbed depend on α

$$\eta = (1 - e^{-\alpha x})$$

- ▶ Wafer with thickness 1 mm suitable for energy upto 20 keV

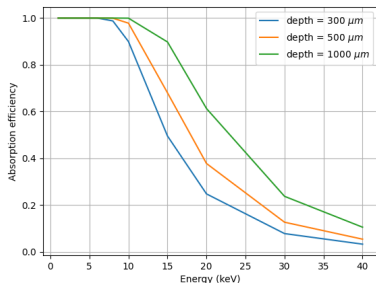
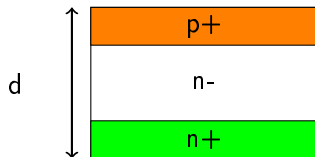


Figure 1: Absorption efficiency increasing with wafer thickness

PIN diode



- ▶ High reverse bias applied to p+ to fully deplete it and generate electric field

$$V_{depletion} = q \frac{N_D d^2}{2\epsilon_{Si}}$$

- ▶ Top and bottom are highly doped to form good ohmic contact
- ▶ High doping also ensures low diffusion current
- ▶ Top p+ and n+ implantation depth are kept small to keep dead volume low

Need for SDD

- ▶ At full depletion, capacitance saturates to a minimum value and is given

$$C = \frac{A\epsilon_s i}{W_{detector}}$$

- ▶ C is proportional to the area which becomes very high for large area detectors. For $A = 50\text{mm}^2$ and $d = 1\text{mm}$, $C \approx 50\text{ pF}$
- ▶ Not suitable for low noise detection

Working of SDD

- ▶ n+ contact can be made small and placed on top
- ▶ Remaining space on top can be covered by p+ to deplete the bulk

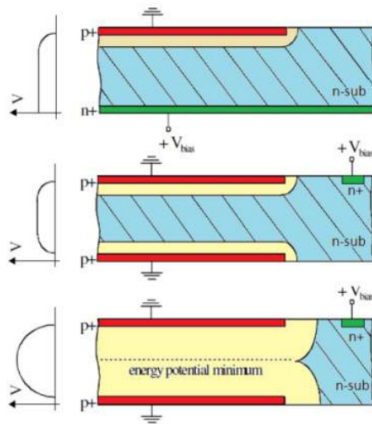


Figure 2: Structure demonstrating sideward depletion.?

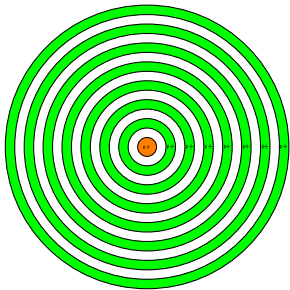


Figure 3: Top view of cylindrical SDD

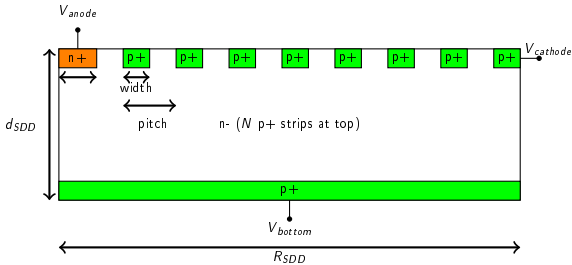


Figure 4: Radial cross-section of cylindrical SDD

Potential gutter

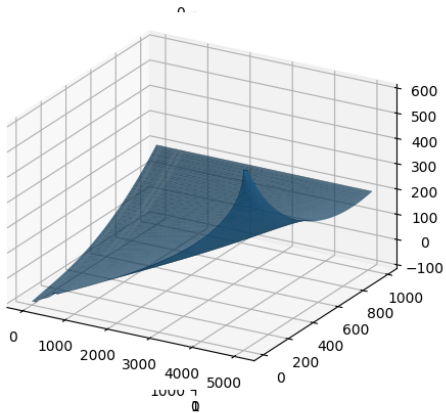


Figure 5: Electron (Negative) Potential in SDD

Goals

For high SNR, C and leakage current should be low.

- ▶ $C < 100 \text{ fF}$
- ▶ Leakage current below 100 nA at room temperature
- ▶ Low drift time (High radial field)
- ▶ Device area = 0.8 cm^2 ($R = 5 \text{ mm}$, $d = 1 \text{ mm}$)

Key Design elements

- ▶ **Anode width:** Decides the anode capacitance
- ▶ **Biasing Range:** Range of allowed bias to maximise field
- ▶ **Surface potential:** Ensure uniform radial drift field

Anode capacitance

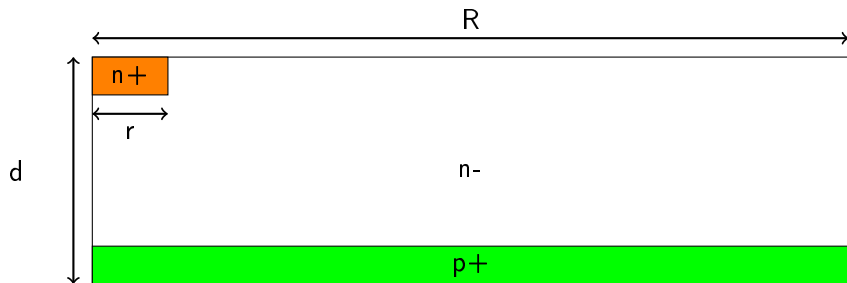
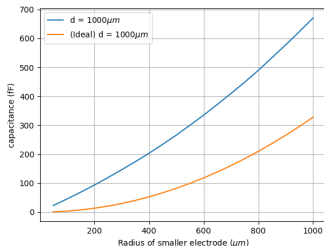


Figure 6: Structure considered for capacitance simulation

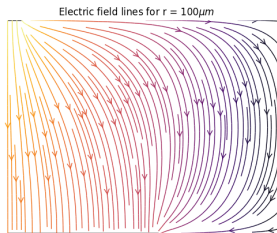
Parallel plate capacitor

$$C = \epsilon \frac{A}{d} = \epsilon \frac{\pi r^2}{d}$$

- ▶ True for $r \gg d$
- ▶ For small r/d , fringing effects become dominant



(a) Real capacitance

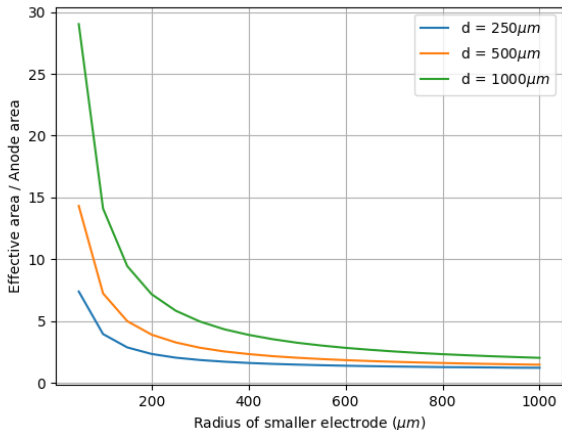


(b) fringe

Parallel plate capacitor

- ▶ Capacitance increase due to fringing is expressed by $A_{effective}$

$$C_{real} = \epsilon \frac{A_{effective}}{d}$$



Parallel plate capacitor

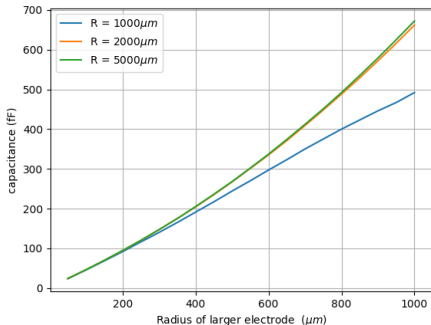


Figure 9: Capacitance is relatively independent of R while d is much smaller than R

- ▶ For large R/d , fringe field don't cross boundary of larger plate
- ▶ Geometric similarity means $\frac{A_{\text{effective}}}{A_{\text{anode}}} = f\left(\frac{r}{d}\right)$

Anode capacitance

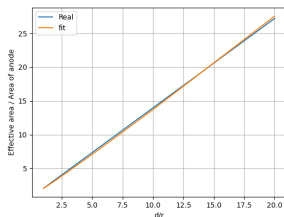


Figure 10: $\frac{A_{\text{effective}}}{A_{\text{anode}}}$ varies linearly with d/r



$$A_{\text{eff}} = A_{\text{anode}} \left(k_1 \frac{d}{r} + k_2 \right)$$

where $k_1 = 1.32$ and $k_2 = 0.73$

- ▶ Anode capacitance about 45 fF for
 $r = 100\mu\text{m}$, $d = 1\text{mm}$, $R = 5\text{mm}$
- ▶ $r = 100\mu\text{m}$ is chosen as anode radius

Material Parameters

- ▶ **Substrate:** n-Silicon $\rho = 10k\Omega - cm$ ($N_D = 5 \times 10^{11}/cm^3$).
 $V_{dep} \approx 380V$
- ▶ **Doping:** Magnitude of doping of $n+$ and $p+$ regions is $10^{18}/cm^3$.
- ▶ **Carrier lifetime:** High-lifetime (>1 ms) Si wafer for low generation current. $\tau_n = \tau_p = 1ms$
- ▶ **Carrier mobility:** $\mu_n = 1000V - cm^2/s$, $\mu_p = 500V - cm^2/s$

Biasing schemes

- ▶ Two possible schemes
- ▶ Voltage divider made by poly-Si resistors on top
- ▶ Intermediate strips left unbiased

Structure with poly-silicon on top

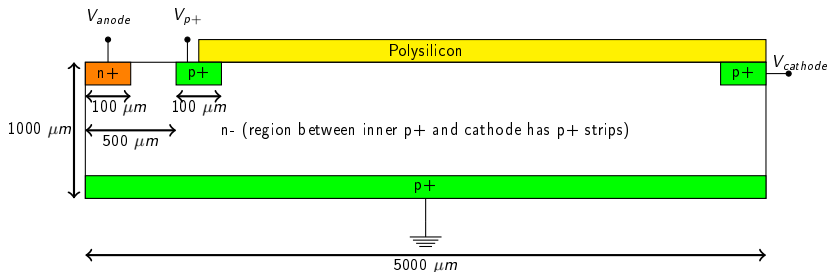


Figure 11: SDD structure considered for simulation (Left edge represent axis of cylindrical structure ($r=0$))[Poly Resistance = 20 ohm/ μm]

Self biased structure

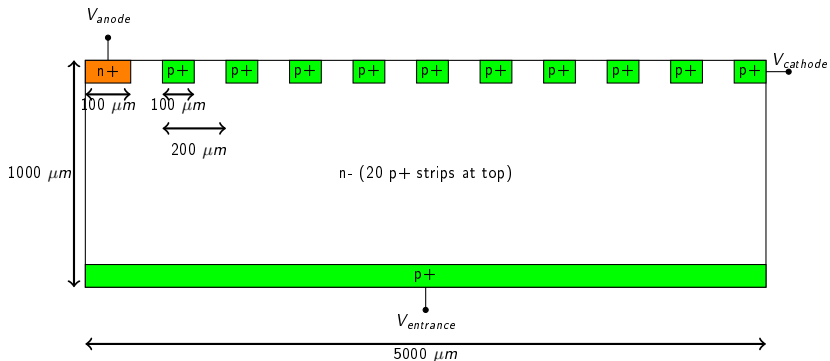


Figure 12: Self-biased SDD structure considered for simulation (there are 25 $p+$ strips at top and shallow $p+$ layer at the entrance)

Depletion

- ▶ High +ve bias to anode, all other electrodes grounded
- ▶ At full depletion, leakage current saturates to 94 nA

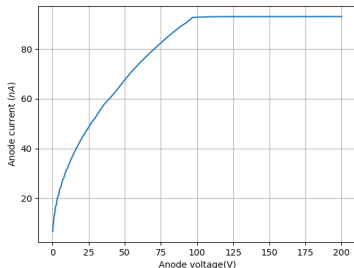


Figure 13: Anode leakage current

- ▶ Leakage current is due to thermal generation (seen by \sqrt{V} relation)

Generating drift field

- ▶ Generate highest drift possible
- ▶ Maintain depletion from breaking
- ▶ Punch through breakdown is the limiting factor

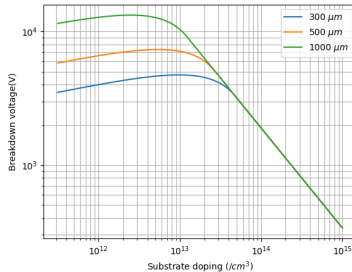


Figure 14: Avalanche breakdown voltage (PIN diode)

Punch through breakdown

- ▶ Consider a vertical section in SDD crossing p+ strip at top and p+ layer at bottom
- ▶ Since whole n- is depleted, both p+-n junctions are reverse biased
- ▶ This is different from punch-through in p-n-p BJTs where one p-n junction is forward biased

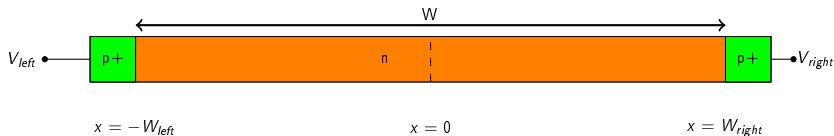


Figure 15: One dimensional section of a p+-n-p structure

Potential profile for p+n-p structure

$$\nabla \cdot \vec{E} = -\frac{d^2 V}{dx^2} = \frac{qN_D}{\epsilon}$$
$$V_{left} \geq V_{right}$$

- ▶ $\frac{qN_D}{\epsilon}$ is the curvature of potential

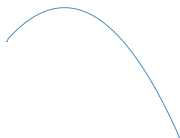


Figure 16: Potential profile of p+n-p structure showing potential barrier for holes (Left end is $x = -W_{left}$ and right end is $x = W_{right}$)

Punch through breakdown

$$\Delta V = V_{left} - V_{right} \quad (1)$$

$$W_{left} = \frac{W}{2} - \frac{\epsilon \Delta V}{q N_D W}; W_{right} = \frac{W}{2} + \frac{\epsilon \Delta V}{q N_D W} \quad (2)$$

- ▶ As +ve bias on left end is increased, the barrier moves towards left and starts decreasing in height
- ▶ Punch-through breakdown occurs when barrier reaches other as barrier becomes small enough

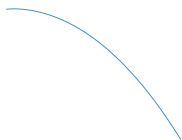


Figure 17: Potential profile of p+-n-p structure showing potential barrier for holes (Left end is $x = -W_{left}$ and right end is $x = W_{right}$)

Punch-through breakdown

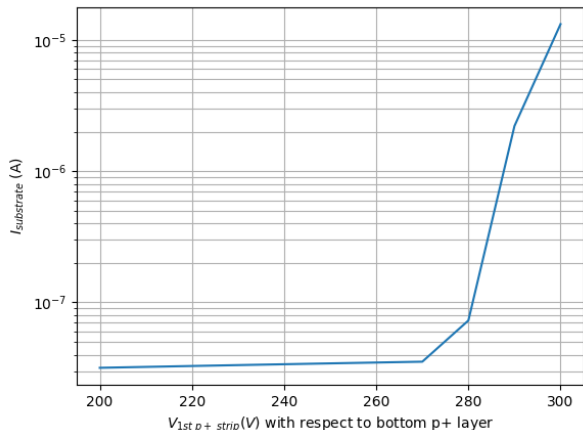


Figure 18: Punch through breakdown occurring at about 270 V difference between inner p+ strip and bottom p+ ($V_{dep} \approx 380V$)
[$V_{n+} = 300V$, $V_{\text{righttop } p+ \text{ strip}} = -350V$, $V_{\text{bottom } p+} = 0V$]

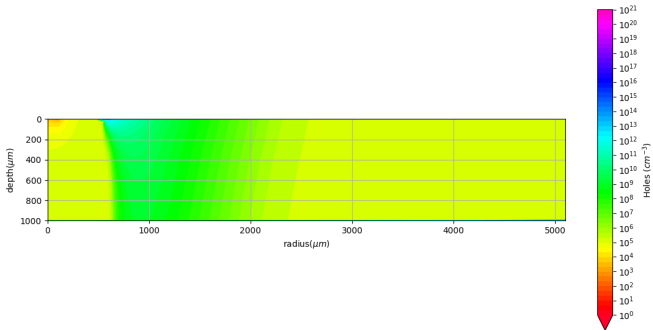


Figure 19: Holes being injected from inner p+ strip breaking down depletion (Voltage difference between top and bottom p+ is 300 V)

Revisiting punch-through breakdown analysis

- ▶ Radial field variation can't be neglected
- ▶ In one-dimensional analysis, all donor dipoles align vertically
- ▶ But, all donor dipoles cannot be completely vertical in presence of radial field

Revisiting punch-through breakdown analysis

$$\nabla \cdot \vec{E} = \frac{1}{r} \frac{\partial(rE_r)}{\partial r} + \frac{\partial E_z}{\partial z} = \frac{E_r}{r} + \frac{\partial E_r}{\partial r} + \frac{\partial E_z}{\partial z} \quad (3)$$

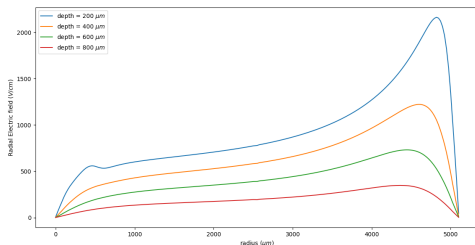


Figure 20: Radial field variation

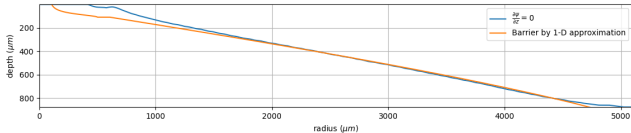


Figure 21: Potential barrier position is more closer to the inner p+ than barrier position given by (??). Potential barrier position is farther from bottom p+ layer than barrier position given by (??). [Barrier position is plotted for structure when breakdown occurs at inner p+.]

Breakdown voltage decreases for inner p+ strip and increase for outer p+ strip

Final bias voltage

- ▶ Voltage divider on top

$$V_{anode} = 300 \text{ V}$$

$$V_{cathode} = -400 \text{ V}$$

$$V_{p+} = 250 \text{ V}$$

$$V_{bottom} = 0 \text{ V}$$

- ▶ Self biased

$$V_{anode} = 350 \text{ V}$$

$$V_{cathode} = -400 \text{ V}$$

$$V_{bottom} = 0 \text{ V}$$

Surface potential

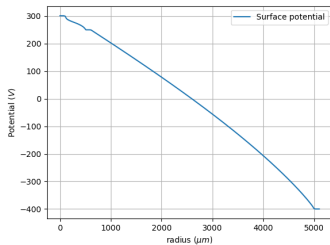
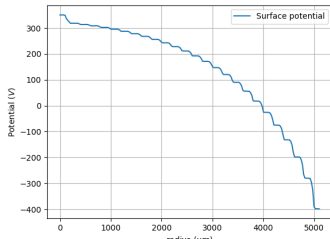


Figure 22: Linear surface potential



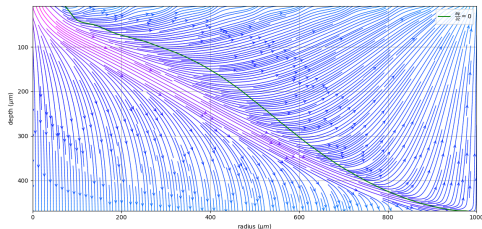
Design Evaluation

- ▶ Radial drift field along
- ▶ Collection efficiency
- ▶ Transient behaviour

Drift channel

- ▶ **Channel** : A pathway for electrons
- ▶ In semiconductors, $\vec{v} \parallel \vec{E}$
- ▶ Center of charge cloud moves along an electric field line
- ▶ Drift channel should be an electric field line
- ▶ Drift path defined by P. Rehak. et. al(1989):

$$\left(\frac{\partial V}{\partial z} \right)_{z=z(r)} = 0$$



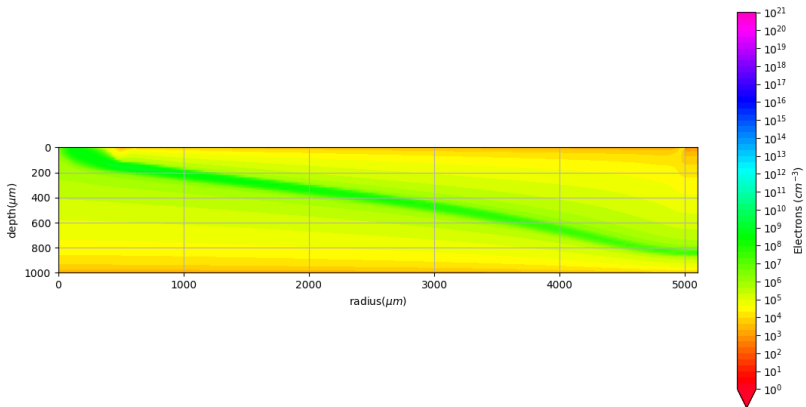
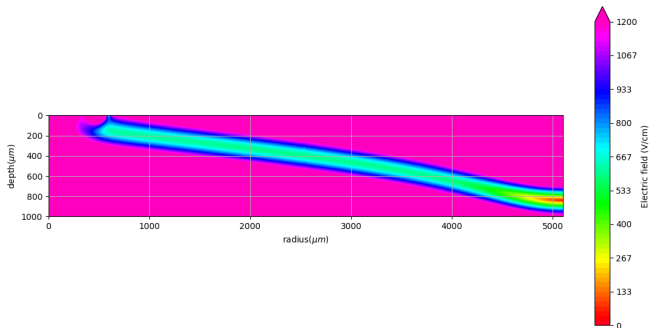
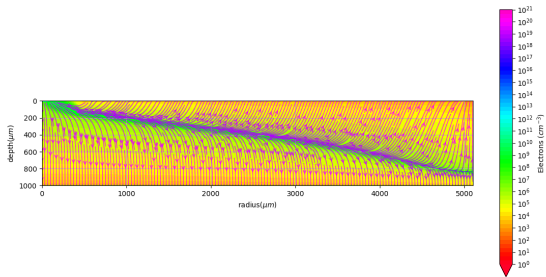
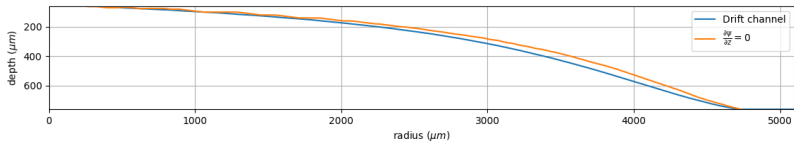


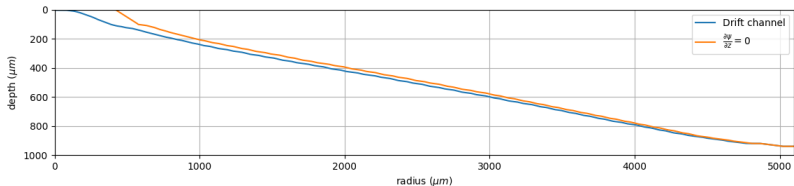
Figure 24: High electron density channel



Drift channel shape



(a) Self-biased surface potential leading to curviest drift channel



(b) Linear surface potential leading to straight drift channel

Figure 25: Drift channel for different surface potentials

Drift time

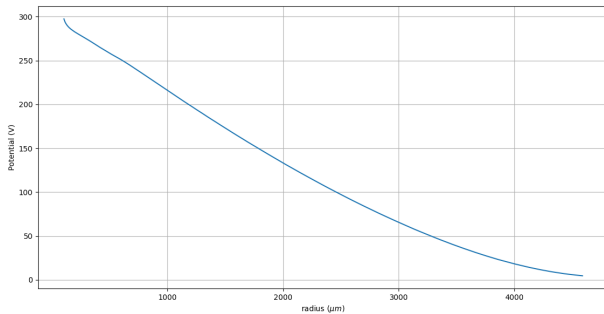


$$t = \int_{r_0}^r \frac{dr}{v_{drift,r}} = \int_{r_0}^r \frac{dr}{\mu_n E_{drift,r}} = \frac{r - r_0}{\mu_n E_{drift,mean}}$$
$$E_{drift,mean} = \frac{r - r_0}{\int_{r_0}^r \frac{dr}{E_{drift,r}}}$$

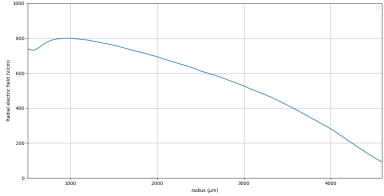
- ▶ Lower electric field regions slow down the carriers and take much of the carrier's drift time
- ▶ Mean drift field closer to minimum electric field than maximum.
- ▶ \implies For a given potential difference, optimum drift field should be uniform

Maximum drift field

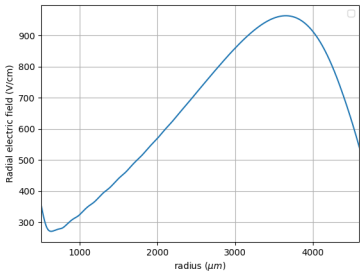
$$(E_{drift,mean})_{max} = \frac{V_{anode} - V_{bottom}}{R}$$



Drift field



(a) Linear surface potential



(b) Self biased surface potential

- ▶ **Straight line potential:** Decreasing field (Low resistance poly)
- ▶ **Self biased potential:** Increasing field (No poly -> Infinite resistance)
- ▶ Optimum in between
- ▶ As channel moves away from n-side (top), effect of surface field diminishes.
- ▶ To counter it, increasing surface field is required.

Surface potential

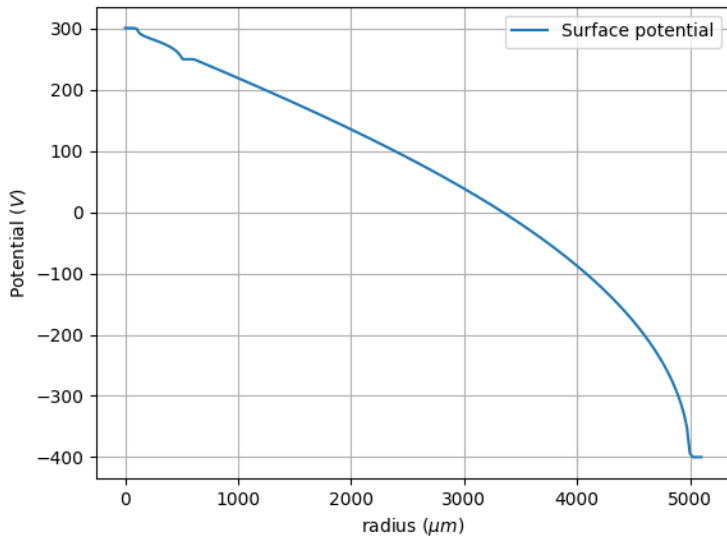


Figure 27: Optimum surface potential

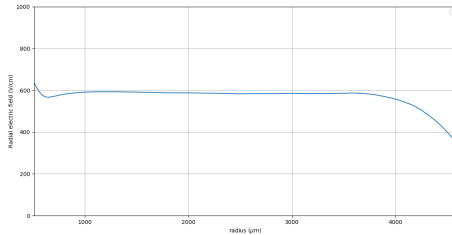


Figure 28: Radial drift field along the channel for curved surface potential

Optimum drift field

$$\phi(r) \propto \left(\sqrt{1 - \frac{r}{R}} - 1 \right)$$

$$z_{dr}(r) = d \left(1 - \sqrt{1 - \frac{r}{R}} \right)$$

$$E_{surface,r} = -\frac{d}{dr}\phi(r) \propto \frac{1}{\sqrt{1 - \frac{r}{R}}}$$

- ▶ Results in uniform radial drift field
- ▶ Diverging electric field at surface

Optimum surface field

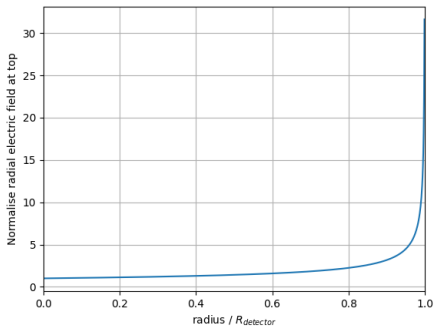
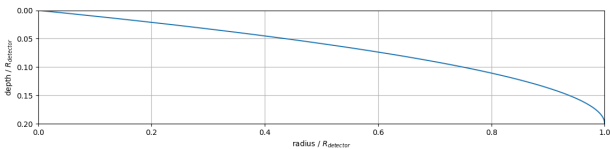


Figure 29: Surface electric field leading to curved optimum drift channel



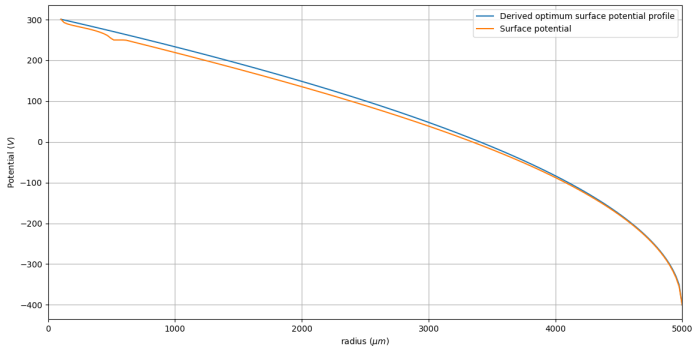
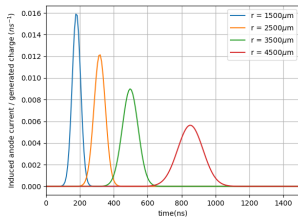


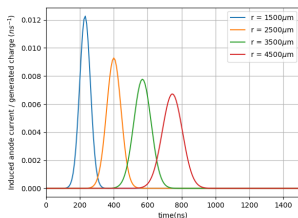
Figure 31: Comparison

Transient pulse

- ▶ Triangular pulse of width 0.1ns incident at different radial distance



(a) Linear Potential



Interpretation using Shockley-Ramo Theorem

$$Q = -q \phi_0(\mathbf{x})$$

$$i = -q \vec{v} \cdot \vec{E}_0(\mathbf{x})$$

- ▶ Weighing potential is a solution of Laplace equation

$$\nabla^2 \phi = 0$$

$$\phi(\text{anode}) = 1, \phi(p + \text{strips}) = \phi(\text{bottom } p + \text{layer}) = 0$$

- ▶ Only depends on geometry of the biased electrodes
(Independent of applied bias and space charge)
- ▶ As charge moves, it gains kinetic energy by energy stored in electric field
- ▶ To restore that, power supplies push more energy which leads to induced charge

Interpretation using Shockley-Ramo Theorem

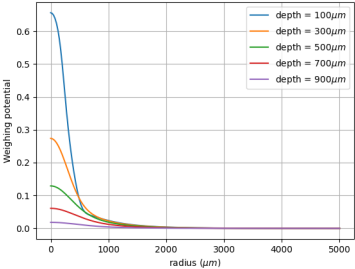
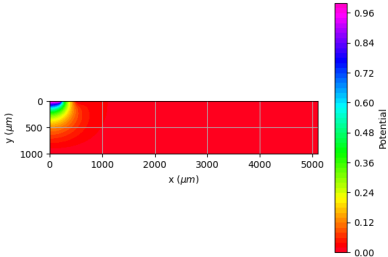
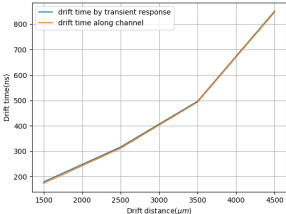
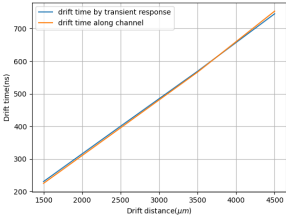


Figure 33: Anode weighing potential at different depths in the detector

Drift time-distance



(a) Linear Potential



(b) Curved Potential

Surface potential	Mean drift field [V/cm] (extracted from transient response)	Mean drift field (by integration)
Curved	604	598
Straight	529	531

Table 1: Mean drift field comparison

Manufacturability

- ▶ Poly-Si resistors: Resistance for optimum case ≈ 49 ohms/ μm
- ▶ For $10 \mu\text{m}$ width, $R_{sheet} \approx 490 \Omega/\text{square}$
- ▶ With 250 nm thickness, doping $\approx 10^{19}/\text{cm}^3$

Summary

- ▶ Linear relation between $A_{effective}/A_{anode}$ and d/r to determine anode radius
- ▶ Analysis of punch through accounting radial flux
- ▶ Drift channel with appropriate definition
- ▶ Mean drift field and Drift time to evaluate device
- ▶ Optimum surface potential by optimising resistance of voltage divider
- ▶ Weighing potential given by S-R theorem to understand induced current on anode
- ▶ SDD of radius 5 mm and depth 1 mm (94 nA, $c \approx 48$ fF and mean drift field of 598 V/cm)

Future Work

- ▶ Design for lower R/d
- ▶ Integrate JFET with SDD
- ▶ Fabricate SDD